Electronic Supplementary Information

Empowering non-covalent hydrogen, halogen and $[S\text{-}N]_2$ bonds in synergistic molecular assemblies on Au(111)

Ana Barragán[1,2,3], Sara Lois[1,4], Ane Sarasola[1,4], Lucia Vitali[1,2,3,5]

1. Donostia International Physics Center (DIPC), Paseo Manuel de Lardizabal 4, 20018 San Sebastian
2. Advanced Polymers and Materials: Physics, Chemistry and Technology, Chemistry Faculty (UPV/EHU), Paseo Manuel de Lardizabal 3, 20018 San Sebastian
3. Centro de Física de Materiales, Centro Mixto CSIC-UPV/EHU, Paseo M Lardizabal 5, 20018 San Sebastian
4. Departamento de Física Aplicada, Universidad del País Vasco (UPV/EHU), E-20018 San Sebastián, Spain
5. Ikerbasque Research Foundation for Science, Plaza Euskadi, 5, Bilbao 48009

ESI1. Experimental and computational methods

The clean Au(111) surface was prepared by cycles of Ar+ ion sputtering and annealing under ultra-high vacuum (UHV) conditions. The Au(111) surface was held at room temperature during the molecular deposition. Then, the sample was transferred within the UHV to the microscope where it was cooled down to 4K to perform STM and STS experiments.

DFT calculations have been carried out using the Vienna Ab Initio Simulation Package (VASP) in its 5.4.4 version [1-3]. The projected augmented wave (PAW) method was used to describe the ion-electron interaction and the electronic exchange and correlation description has been done by means of the Perdew, Burke, and Ernzerhof (PBE) functional within the generalized gradient approximation (GGA) [4]. Dispersion forces have been included self-consistently via the vdW-dF2 method in its optB88-vdW approximation [5].

Periodic conditions have been imposed to all of our systems optimizing the atomic positions up to forces weaker than 0.01 eV/Å. The size and orientation of the unit vectors were allowed to relax together with the atomic positions. The energy convergence criterion was of 10^{-4} eV. Those conditions assure sufficient accuracy in the numerical values of the calculated magnitudes. The Kohn-Sham orbitals were expanded in a plane wave basis set with a kinetic energy cutoff of 400 eV for all the systems considered and a Γ point k-point sampling was used.

Once systems were relaxed and self-consistent charge distribution was obtained, Bader charges, projected density of states and local density of states were obtained by the post-processing of the electronic files.

ESI2: Adsorption of dimers on Au(111)

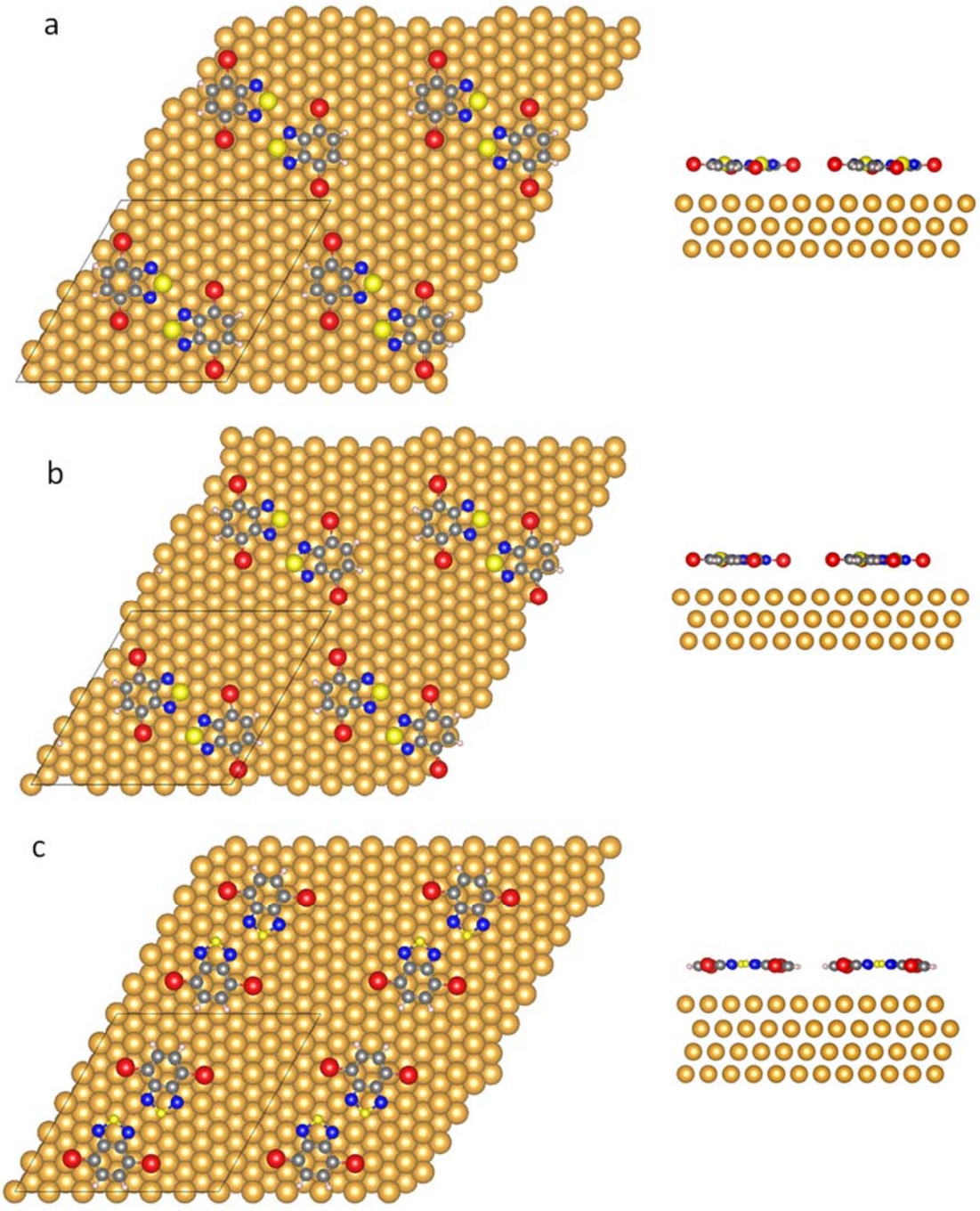

Figure ESI1. Calculated top and side view adsorption geometries for a 2Br-BTD dimer on top of Au(111). **a.b**. The backbone of the molecules is parallel to the [1-12] direction of the surface, with different atomistic registry. **c.** The backbone of the molecules is parallel to the [110] direction of the surface

Figure ESI1 shows different geometries considered to calculate the molecular interaction with the supporting substrate by Density Functional Theory. The substrate has been simulated by using 6x6 unit cells and 3 or 4 layers of Au together with 5 layers of vacuum

to assure the lack of interaction between the adsorbed dimers and/or the periodic cells. Panels **a** and **b** correspond to two different stacking registries of the molecules with respect to the Au(111) atomic structure along the [1-12] symmetry direction. Instead in panel **c.** the molecules orient along the [110] high symmetry direction of Au(111). Only in the first two configurations, the molecular backbone orients according to the experimental evidence. The calculated adsorption energies E_{ads} are: **a**= -265meV and **b**= -282meV, respectively. The small and comparable values are indicative of the weak interaction, where the Au(111) surface shows weak influence on the molecular registry.

This weak interaction is confirmed also by the relatively large adsorption vertical distances of the molecular dimers. We took S atoms as a reference and in the configurations **a., b**. and **c.** S atoms are 4.25Å 4.08Å 4.37Å apart from the surface, respectively, which are large enough to confirm the almost negligible interaction between the dimers and the surface. Å. Besides, the in-plane intermolecular distance between Sulfur and Nitrogen atoms calculated for an absorbed $[S\text{-}N]_2$ synthon in those three tested configurations are about a. 3.22Å, b. 3.24Å and c. 3.21Å respectively. Thus comparable, though slightly larger than the one of the freestanding dimer that is 3.18Å, discussed in the main paper. This piece of evidence supports the hypothesis of weak adsorbate-substrate interaction, thus allowing the simplification of the calculations considering only the freestanding metal organic P1 and P2 systems.

ESI3. Supramolecular structure characteristics

ESI3a: Structural information

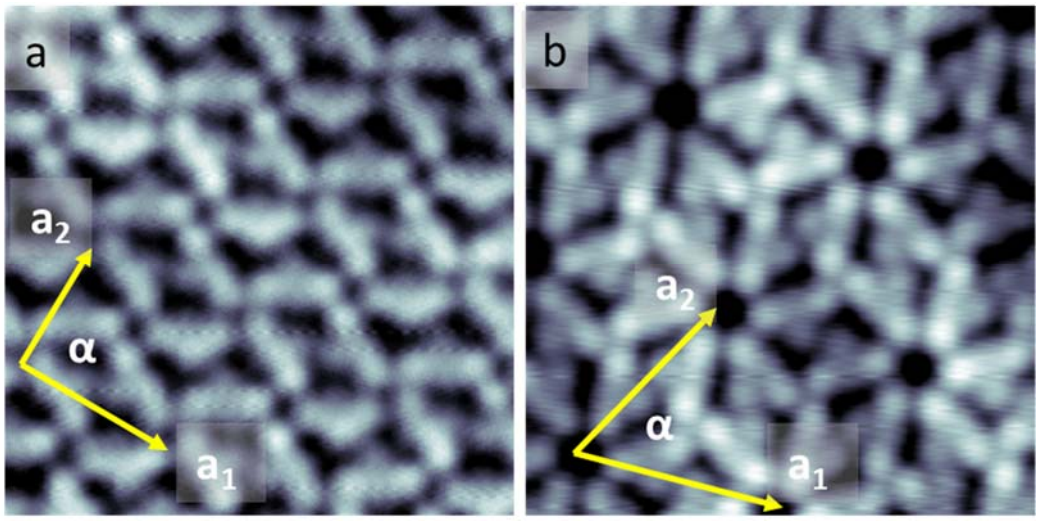

Figure ESI2. Structure of the two molecular assemblies. a. P1 and **b.** P2 networks. The unit cell vectors, identified by the arrow, indicate the structure periodicity in the two phases.

Figure ESI2 indicates the unit cell size of the two molecular phases. The plotted vectors identify the P1 (2-fold symmetry) and P2 (3 fold symmetry) periodicity, which contain 4 molecules, for a molecular density of 1.67nm^{-2}(P1), and 6 molecules for a molecular density of 1.73nm^{-2} (P2), respectively.

These cells were calculated with first principle methods allowing the unit cell shape, volume and the ions to relax. The results of these structures are shown in figure 2 c and d of the main manuscript, while the corresponding lattice constants, summarized in Table ESI1, show an excellent agreement with the experimental values.

Unit cell parameters	**a_1 (Å)**	**a_2 (Å)**	**A (º)**
P1 experimental	16.5 ± 1	14.5 ± 1	90 ± 5
P1 theoretical	16.8	13.9	
P2 experimental	20 ± 1	20 ± 1	60 ± 5
P2 theoretical	20.4	20.4	

Table ESI1. Comparison between the experimental and the theoretical lattice parameters for the two phases, P1 and P2.

ESI3b: Chirality

The assembly of P1 and P2 networks have in common the formation of dimer pairs through the interaction of sulfur and nitrogen atoms in the thiadiazole groups of the two facing molecules. The formation of this $[S\text{-}N]_2$ heterocycle confers a chiral character to the dimer (Figure ESI3), which is transferred in the two networks. In the P1 structure, both chiral directions are visible in the same domain of the network. Instead, in the P2 phase, each domain shows either of the two chiralities. However, both of them are observed, with equal probability across the surface.

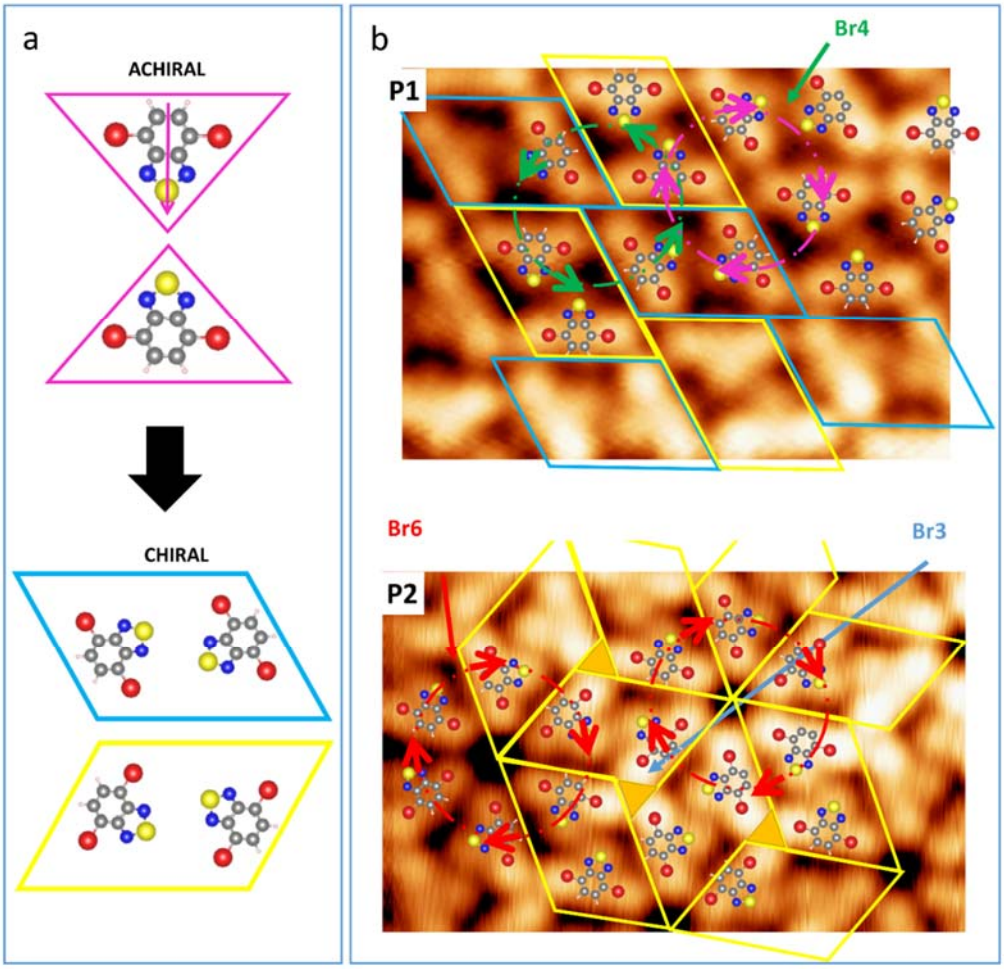

Figure ESI3. Chirality in the two molecular networks. **a**. Chiral character of the dimeric structure in the $[S\text{-}N]_2$ synthon. **b-c.** Chirality in P1 (upper image: 4.1nm x 3.0nm, 0.3V, 600pA) and P2 (bottom image: 5.0nm x 3.1nm, -0.05V, 1nA) structures, respectively.

ESI3c: Secondary bond interaction: halogen-halogen bond and bromine synthon structures

The high directionality of the halogen-halogen bonds derives from the so-called □-hole, i.e., an electron depleted atomic area that characterizes pnicogen, chalcogen and halogen bonded atoms[6-7]. Under such forces, the molecules orient in such a way that their Br terminations interact with each other through electrostatic dipolar attractions, forming characteristic molecular synthons, where the electron-poor region of each molecule points towards the electron-rich atomic side of the neighboring molecule. In our systems, the halogen-halogen interaction favors three different types of nodal configurations, as sketched in figure ESI4. In the P1 network, four molecules interact forming a Br_4 synthon. Instead, the P2 structure holds two Br_3 synthons in each unit cell and one Br_6 synthon. Each of these nodal structures results in a clearly defined angle between the molecules, as shown in figure ESI4 and summarized in table ESI2.

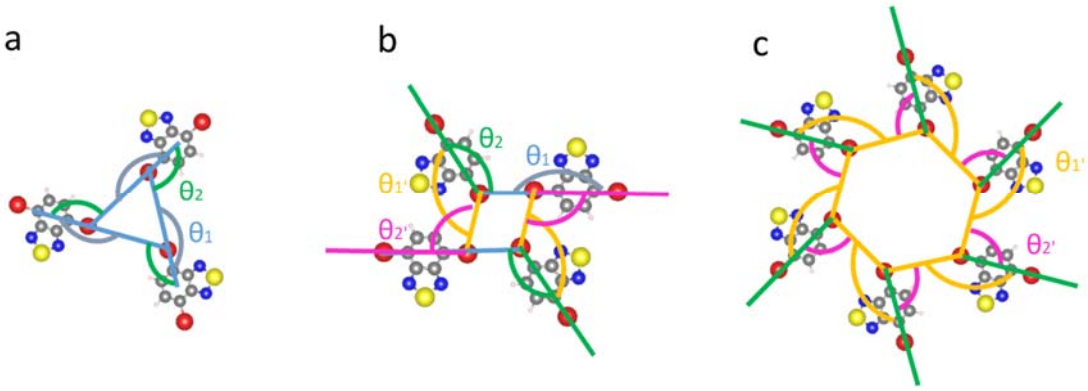

Figure ESI4. Observed bonding angles between Br atoms interaction. a. Br_3 synthon between three molecules **b.** Br_4 **c.** Br_6. The color code highlights the relative orientation of the molecules within the synthons.

	Br3 (P2)	Br4 (P1)	Br6 (P2)
θ_1	180º	180º	
θ_2	120º	124º	
θ_1		133º	150º
θ_2		102º	90º

Table ESI2: Measured angles for each Br arrangement for both phases, P1 and P2.

ESI4: Bond-distances in isolated synthons and networks

For their relevance in the correct understanding of the message of this work, we detail, in this section, the intermolecular distances described in Table 1 and Figure 3 of the main manuscript.

ESI4a: Bond distances in isolated synthons:

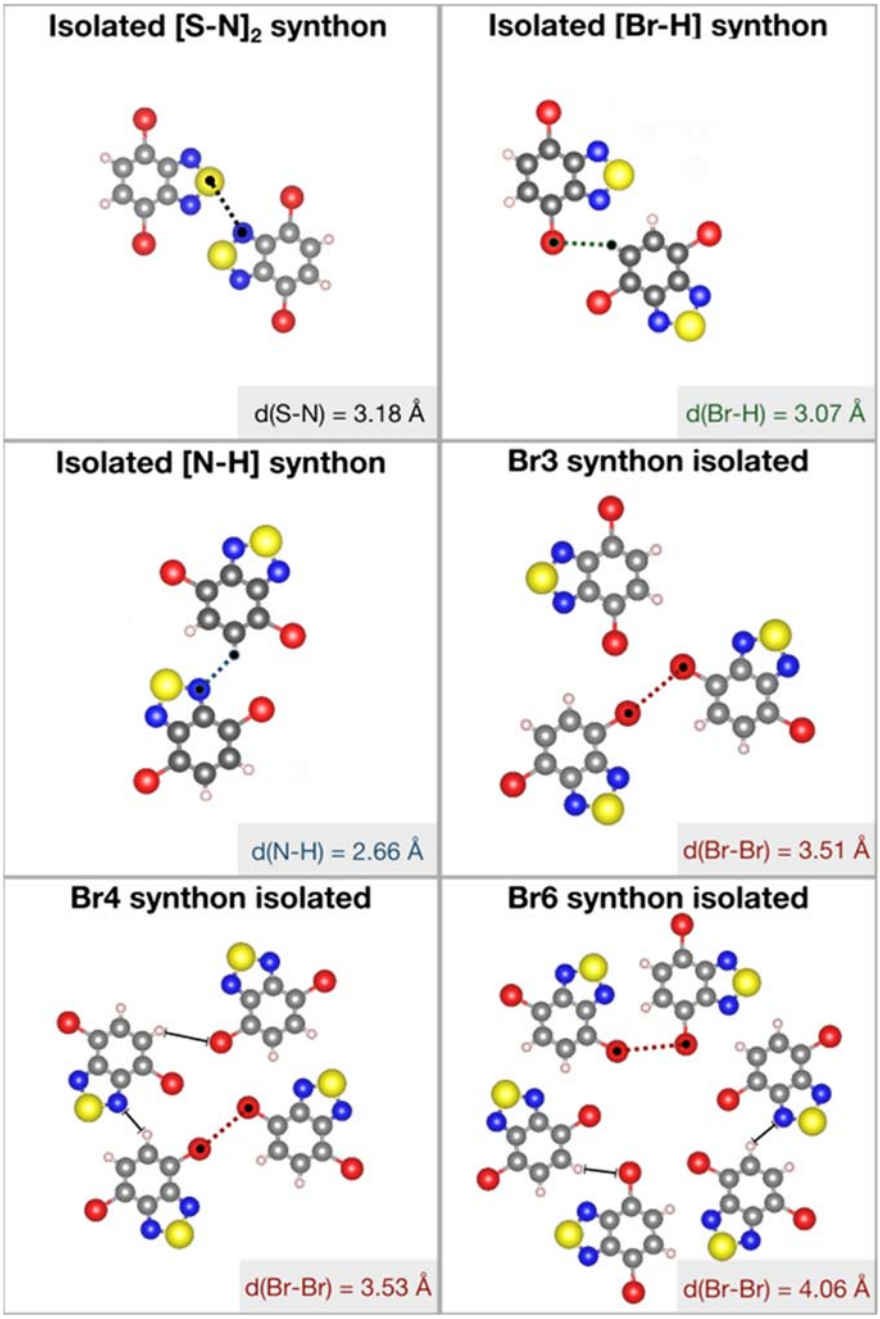

Fig. ESI5: **Six isolated synthons and calculated equilibrium distances**. The continuous and dashed lines highlight some of the secondary interactions as S-N, Br-H, N-H and Br-Br, observed in the P1 and P2 networks. Black lines indicate those bonds that could oppose to further reduction of the Br-Br distance in the synthon.

ESI4b: Calculated network structures and interatomic distances

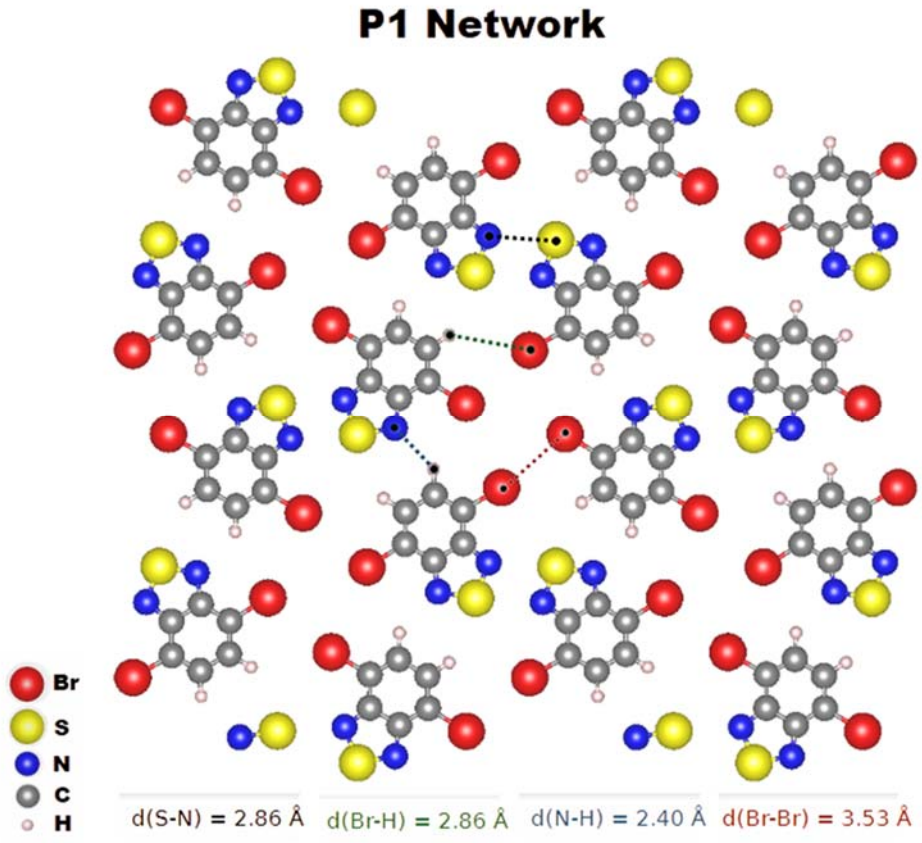

Fig. ESI6: The equilibrium distances calculated for the P1 network.

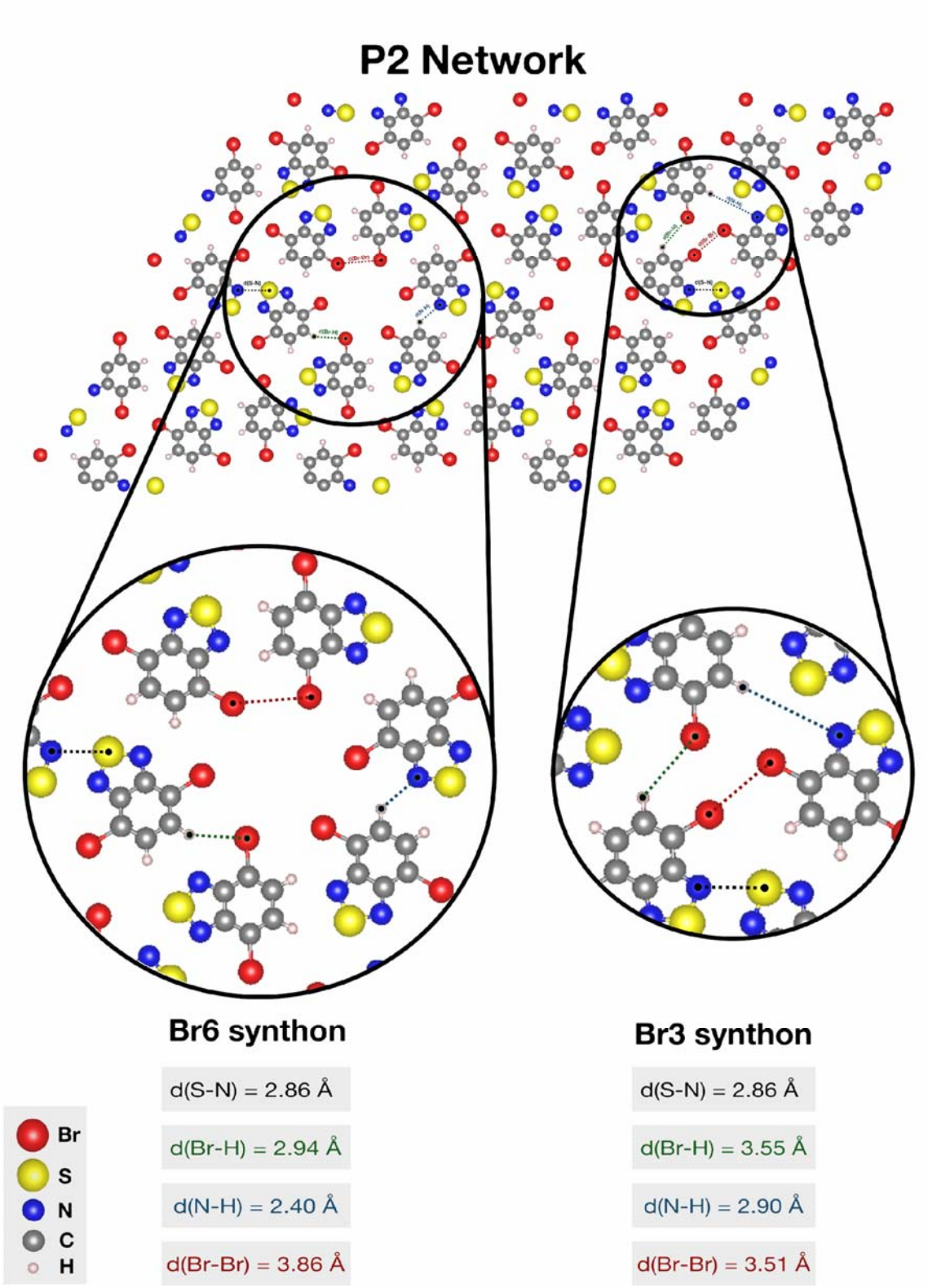

Fig. ESI7: The equilibrium distances calculated for the P2 network.

ESI4c: Experimental network distances

A mean value of interatomic distances can be obtained from high-resolution experimental topographic images. Figure ESI8 shows two prototypical height profiles measured along the S-N and Br-Br directions. Table ESI3 reports the mean bond length averaged over multiple positions. It is worth noting that these experimental values are in full agreement with the values predicted by Density Functional Theory for the two assembled layers given in Table 1 of the main manuscript confirming the shrinkage of the S-N bond whilst P1 and P2 networks are formed.

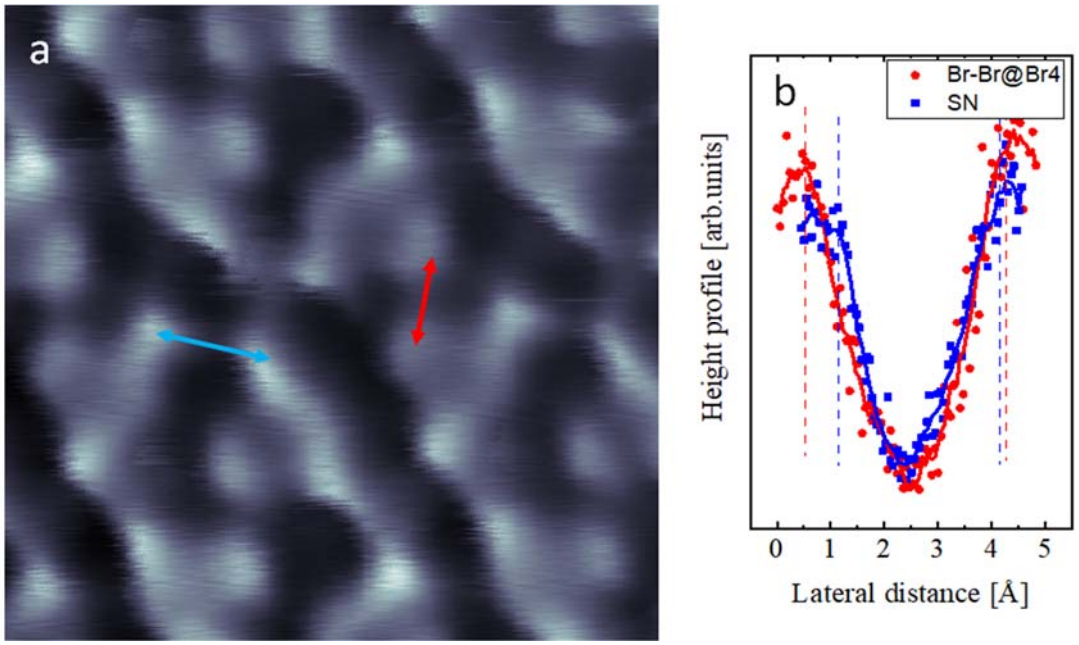

Figure ESI8. Experimentally observed intermolecular distances a. Constant height image showing sub-molecular resolution (Sample bias: 2mV; Image size: 2.5x2.5nm). **b**. Estimate of the intermolecular distances from line profiles along the S-N and Br4 synthons, as indicated by the arrows in panel a.

Mean experimental interatomic distances along specific 2Br-BTD secondary bond interaction [Å]:	
[S-N]2	2.86±0.13
Br-Br in Br3 synthon	3.49±0.12
Br-Br in Br4 synthon	3.56±0.16
Br-Br in Br6 synthon	3.77±0.10

Table ESI3: Mean experimental interatomic distances along selected secondary bond interactions.

ESI5: Induced charge density in the secondary bonds

The map of the induced charge density shows the charge redistribution around the secondary bonds in the formation of the networks. Figure 4 of the main manuscript shows that the main contribution of the induced charge density localized around the $[S\text{-}N]_2$ bonding. In figure ESI9, we highlight the induced charge density at the other interacting position of the molecules in the P1 and P2 phases. At this aim, the electronic charge density of 2 (3) pairs of isolated dimers has been subtracted to the total electronic density in a P1 (P2) unit cell, respectively. Consistently, with the results of the Table 1 of the main manuscript, as figure ESI9 highlights the induced charge density of P1 focuses mainly around N-H surroundings, whereas in the P2 case, the largest contributions are centered on the N-H and Br-H bondings close to Br6 synthon.

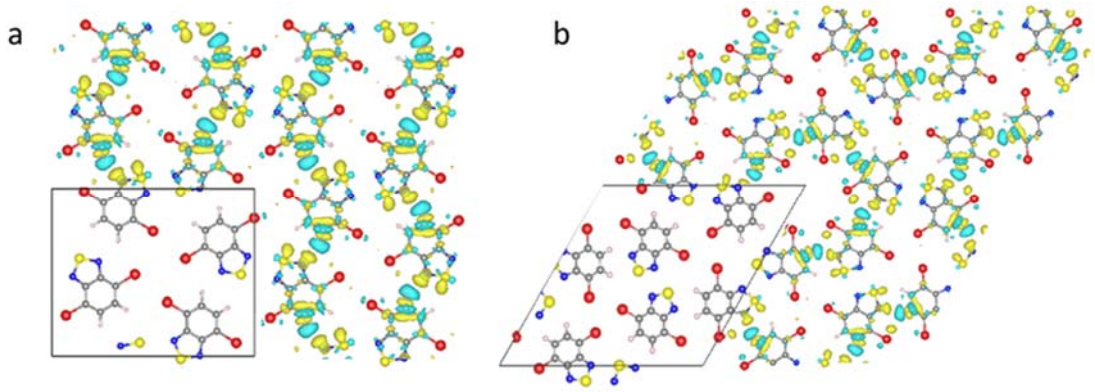

Figure ESI9. Induced charge density of P1 and P2 networks with respect to the dimeric structure. The induced charge density of the dimer shown in Figure 4 of main text has been subtracted to the dimeric pairs included in the P1 and P2 structures.

ESI6. References

(1) G.Kresse, J.Hafner, Phys. Rev. B 1993, 47, 558-561
(2) G. Kresse, J.Furthmüller, Phys. Rev. B, 1996, 54, 11169-11186
(3) G.Kresse, J.Furthmüller, Comput. Mater. Sci. 1996 6, 15-50
(4) J. P. Perdew, K.Burke, M.Ernzerhof, Phys. Rev. Lett. 1997 78, 1396-1396
(5) J.Klime, D. R Bowler, A.Michaelides, J. Phys. Condens. Matter 2010 22, 022201
(6) Oliveira V., Kraha E., Systematic Coupled Cluster Study of Noncovalent Interactions Involving Halogens, Chalcogens, and Pnicogens *J.Phys. Chem A*. **2017**, 121, 9544
(7) Dominikowska J., Rybarczyk-Pirek A.J., Fonseca Guerra C., Lack of cooperativity in the triangular X3 halogen bonded Synthon? *Crys. Growth Des*. **2021**, 21, 597-607